THE JOURNAL OF BIOLOGICAL CHEMISTRY Vol. 278, No. 6, Issue of February 7, pp. 4057–4062, 2003

Printed in U.S.A.

ω-Conotoxin CVID Inhibits a Pharmacologically Distinct Voltage-sensitive Calcium Channel Associated with Transmitter Release from Preganglionic Nerve Terminals*

Received for publication, September 30, 2002, and in revised form, November 15, 2002
Published, JBC Papers in Press, November 18, 2002, DOI 10.1074/jbc.M209969200

David J. Adams‡§, Amanda B. Smith‡, Christina I. Schroeder‡¶, Takahiro Yasuda‡, and Richard J. Lewis‡¶

From the ‡School of Biomedical Sciences and ¶Institute for Molecular Bioscience, The University of Queensland, Brisbane, Queensland 4072, Australia

Neurotransmitter release from preganglionic parasympathetic neurons is resistant to inhibition by selective antagonists of L-, N-, P/Q-, R-, and T-type calcium channels. In this study, the effects of different ω-conotoxins from genus *Conus* were investigated on current flow-through cloned voltage-sensitive calcium channels expressed in *Xenopus* oocytes and nerve-evoked transmitter release from the intact preganglionic cholinergic nerves innervating the rat submandibular ganglia. Our results indicate that ω-conotoxin CVID from *Conus catus* inhibits a pharmacologically distinct voltage-sensitive calcium channel involved in neurotransmitter release, whereas ω-conotoxin MVIIA had no effect. ω-Conotoxin CVID and MVIIA inhibited depolarization-activated Ba^{2+} currents recorded from oocytes expressing N-type but not L- or R-type calcium channels. High affinity inhibition of the CVID-sensitive calcium channel was enhanced when position 10 of the ω-conotoxin was occupied by the smaller residue lysine as found in CVID instead of an arginine as found in MVIIA. Given that relatively small differences in the sequence of the N-type calcium channel α_{1B} subunit can influence ω-conotoxin access (Feng, Z. P., Hamid, J., Doering, C., Bosey, G. M., Snutch, T. P., and Zamponi, G. W. (2001) *J. Biol. Chem.* 276, 15728–15735), it is likely that the calcium channel in preganglionic nerve terminals targeted by CVID is a N-type ($Ca_v2.2$) calcium channel variant.

Venom of the predatory marine gastropods of the genus *Conus* (cone snails) contain a unique array of peptides whose pharmaceutical potential remains largely unexploited (1). These peptides have been classified based on their pharmacological target and structure (2, 3). One important class, the ω-conotoxins, utilizes a four-loop framework to selectively inhibit "N-type" voltage-sensitive calcium channels (VSCCs)[1] found in the central and peripheral nervous systems of vertebrates (4).

Neurotransmitter release from preganglionic parasympathetic neurons has been found to be resistant to inhibition by a range of selective calcium channel antagonists of L-, N-, P/Q-, R-, and T-type calcium channels (5–8). A recently discovered ω-conotoxin from *Conus catus* (CVID) is highly selective for N-type over P/Q-type VSCCs (9) and shows potent analgesic activity in rats (10). In this study, we investigated the effects of CVID on autonomic neurotransmission using conventional intracellular microelectrode recording techniques. ω-Conotoxin CVID was found to be a potent inhibitor of neurally evoked transmitter release from the intact preganglionic cholinergic nerves innervating the rat submandibular ganglia, whereas ω-conotoxin MVIIA had no effect.

The orientation and nature of the residues in loop 2 of ω-conotoxins have been shown to be crucial for selective binding to the N-type VSCC (11–15). Since the only sequence difference in loop 2 between CVID and MVIIA is at position 10, we investigated the importance of this position for ω-conotoxin structure and ability to block neurotransmitter release from preganglionic parasympathetic neurons. The inhibition of preganglionic transmitter release was favored in ω-conotoxins with a Lys at position 10.

EXPERIMENTAL PROCEDURES

Submandibular Ganglia Preparation—2–5-week-old rats were anesthetized and killed by cervical fracture prior to the removal of the submandibular ganglia in accordance with the guidelines of the University of Queensland Animal Experimentation Committee. The submandibular ganglia were removed as described previously (8, 16). Individual preparations were pinned to the Sylgard (Dow Corning) covered base of a 2-ml Perspex organ bath. Preparations were continuously perfused at a rate of 2 ml/min with a Krebs phosphate solution of the following composition (in mM): 118.4 NaCl, 25.0 $NaHCO_3$, 1.13 NaH_2PO_4, 1.8 $CaCl_2$, 4.7 KCl, 1.3 $MgCl_2$, and 11.1 glucose, gassed with a mixture of 95% O_2 and 5% CO_2 to pH 7.4, and maintained at 36–37 °C.

Intracellular Recordings and Analysis—The lingual nerve was field-stimulated by voltage pulses via bare platinum wires delivered from a digital stimulator (Pulsar 7^+, Frederick Haer & Company, Brunswick, ME) coupled to an optically isolated stimulation unit (Model DS2, Digitimer Ltd., Welwyn Garden City, United Kingdom). Intracellular recordings were made from individual ganglion cells using glass microelectrodes filled with 5 M potassium acetate (resistances 70–120 megohms). Conventional intracellular recording techniques were used as described previously (17, 18). Membrane potentials were recorded through a headstage connected to an Axoclamp-2A amplifier (Axon Instruments Inc., Union City, CA) in bridge mode and stored on a digital audio tape using a digital tape recorder (DTR-1204, BioLogic Science Instruments, Claix, France). Evoked events were digitized at 5–10 kHz and transferred to a computer using an analogue-to-digital converter (Digidata 1200A interface) and Axotape software (Axon Instruments Inc.). The amplitude, frequency, rise time, and latency of evoked and spontaneous events were analyzed using Axograph 2 (Axon Instruments Inc.). The mean resting membrane potential of the sub-

* This work was supported in part by the Australian Research Council and National Health and Medical Research Council of Australia. The costs of publication of this article were defrayed in part by the payment of page charges. This article must therefore be hereby marked "*advertisement*" in accordance with 18 U.S.C. Section 1734 solely to indicate this fact.

§ To whom correspondence should be addressed: School of Biomedical Sciences, University of Queensland, Brisbane, QLD 4072, Australia. Tel.: 61-7-3365-1074; Fax: 61-7-3365-4933; E-mail: dadams@mailbox.uq.edu.au.

[1] The abbreviations used are: VSCC, voltage-sensitive calcium channel; EPSP, excitatory postsynaptic potential; HBTU, 2-(1H-benzotriazol-1-yl)-1,1,3,3-tetramethyluronium hexafluorophosphate; BAPTA, 1,2-bis(*O*-aminophenoxyl)ethane-*N*,*N*,*N*′,*N*′-tetraacetate.

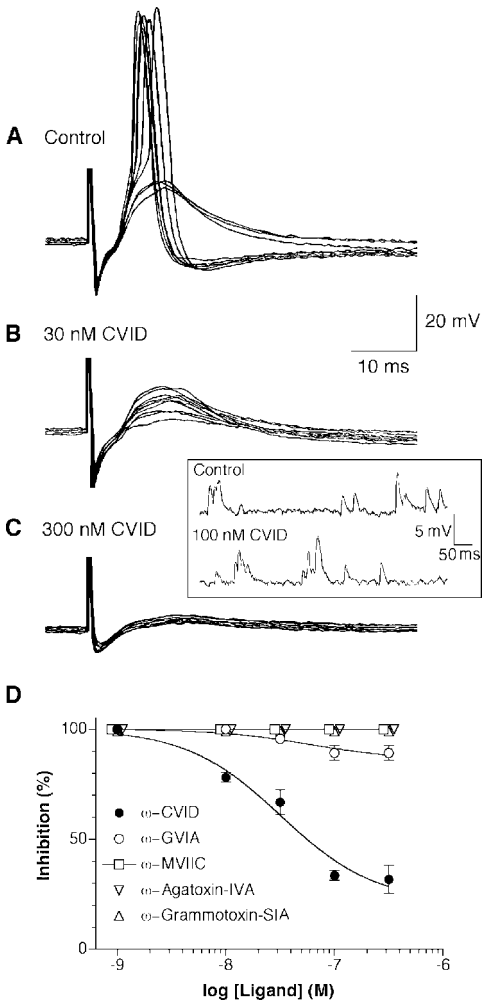

FIG. 1. **Effect of ω-conotoxin CVID on nerve-evoked EPSPs and spontaneous EPSPs in the rat submandibular ganglion.** *A*, control EPSPs evoked by trains of 10 stimuli at 1 Hz. *B*, postsynaptic responses evoked 20 min after the bath application of 30 nM CVID. *C*, postsynaptic responses evoked 20 min after the bath application of 300 nM CVID. *Inset*, effect of CVID (100 nM) on spontaneous EPSPs. *D*, dose-response relationship obtained for the effects of the calcium channel antagonists, ω-conotoxin CVID, ω-conotoxin GVIA, ω-conotoxin MVIIA, ω-grammotoxin SIA, and ω-agatoxin IVA on EPSP peak amplitude. The *solid lines* represent the best fit of the data for each toxin.

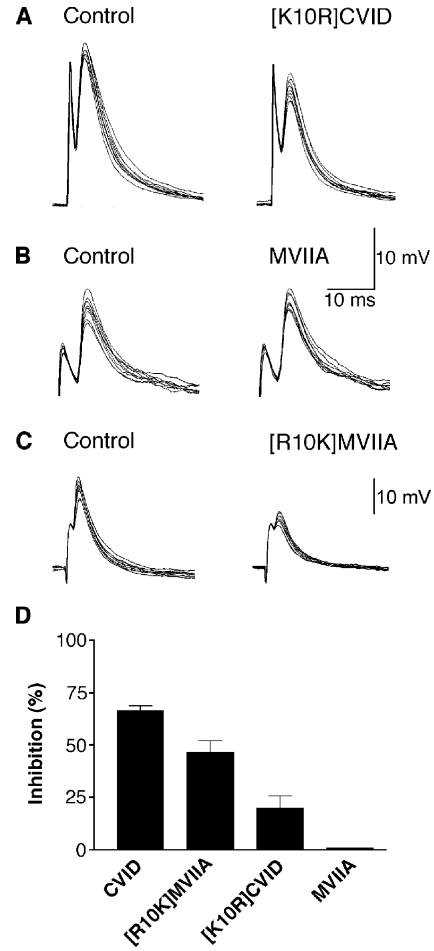

FIG. 2. **Effect of [K10R]CVID, ω-conotoxin MVIIA, and [R10K]MVIIA on EPSPs in the rat submandibular ganglion.** EPSPs were evoked by trains of 10 stimuli at 0.5 Hz. *A*, 10 superimposed traces in the absence (*control*) and presence of 100 nM [K10R]CVID. *B*, 10 superimposed traces in the absence (*control*) and presence of 100 nM MVIIA. *C*, 10 superimposed traces in the absence (*control*) and presence of 100 nM [R10K]MVIIA. *D*, histogram of the percentage inhibition of EPSP amplitude by equivalent concentrations (100 nM) of CVID, [K10R]CVID, MVIIA, and [R10K]MVIIA.

mandibular ganglion neurons was −63.8 ± 0.6 mV (n = 52). The mean base line was determined by averaging the initial part of the digitized signal between the stimulus artifact and the onset of the response. Data are expressed as the mean ± S.E., and n values refer to the number of preparations. Data were analyzed statistically using Student's paired t test with the level of significance being taken as $p < 0.05$.

Electrophysiological Recording of Recombinant Ca^{2+} Channel Currents in Xenopus Oocytes—Capped RNA transcripts encoding full-length rat α_{1B} and β_3 (a gift of D. Lipscombe, Brown University) and rabbit α_{1C} and $\alpha_2\delta$ (a gift of G. Zamponi, University of Calgary) were synthesized using a mMESSAGE mMachine *in vitro* transcription kit (Ambion). *Xenopus laevis* stage V–VI oocytes were removed and treated with collagenase (Sigma type I) for defolliculation. For N- or L-type Ca^{2+} channel expression, the oocytes were then injected with cRNA mixtures of either α_{1B} (2.5 ng/cell) or α_{1C} (5 ng/cell) in combination with $\alpha_2\delta$ and β_3 in the ratio of 1:1:1 or 1:2.5:1, respectively. For R-type Ca^{2+} channels, cDNA for rat α_{1E} (4.5 ng/cell) (a gift of G. Zamponi, University of Calgary) was injected intranuclearly in combination with the cRNA injection of $\alpha_2\delta$ and β_3 (2.5 ng/cell each). The oocytes were incubated at 18 °C in ND96 solution (in mM): 96 NaCl, 2 KCl, 1 $CaCl_2$, 1 $MgCl_2$, 5 HEPES, 5 pyruvic acid, and 50 μg/ml gentamicin, pH 7.5, prior to recording. 3–8 days after cRNA/cDNA injection, whole cell Ca^{2+} channel currents were recorded from oocytes using the two-electrode (virtual ground circuit) voltage clamp technique. Microelectrodes were filled with 3 M KCl and typically had resistances of 0.3–1.5 megohms. All recordings were made at room temperature (20–23 °C) using bath solution containing the following components (in mM): 5 $BaCl_2$, 85 tetraethylammonium hydroxide, 5 KCl, and 5 HEPES titrated to pH 7.4 with methansulfonic acid. During recording, oocytes were perfused continuously at a rate of ~1.5 ml/min. The activation of Cl^- current by Ba^{2+} influx through the Ca^{2+} channel was eliminated by injecting 50 nl of 50 mM BAPTA-Na_4 at least 15 min prior to recording. Using a GeneClamp 500B amplifier and pCLAMP 8 software (Axon Instruments Inc.), data were acquired at 10 kHz after low pass filtration at 1 kHz and leak-subtracted on-line using a P/4 protocol and analyzed. Currents were evoked with 100-ms depolarizing pulses to 0 mV from a holding potential of −80 mV at 20-s intervals. Peak current was measured before and during the perfusion of ω-conotoxins and antagonists for up to 10 min.

Radioligand Binding—Preparation of rat brain membrane and [^{125}I]GVIA and radioligand displacement protocols were as described previously (9, 14, 15).

ω-Conotoxin Synthesis—ω-Conotoxins CVID, [K10R]CVID, MVIIA, [R10K]MVIIA, and [Y13F]CVID were assembled by manual stepwise synthesis using *in situ* neutralization with Boc chemistry (19). Starting from methylbenzhydrylamine HCl resin (0.5-mmol scale), 4 eq of Boc-protected amino acids were coupled to the growing chain using 4 eq of 0.5 M HBTU in *N*′,*N*′-dimethylformamide and 5 eq of *N*,*N*-diisopropylethylamine. The side chain protection chosen was Arg(Tos), Asp(O-cHex), Lys(CIZ), Thr(Bzl), Tyr(BrZ), Ser(Bzl), and Cys(p-MeBzl). The chain assembly was monitored after each step by the quantitative ninhydrin method and double-coupled when coupling yields were <99.7%. The capping of the remaining amino groups by acetylation was

TABLE I
Sequences and potency[a] of synthetic ω-conotoxins
CVID, a conotoxin from *Conus catus*; MVIIA, a conotoxin from *Conus magus*; GVIA, a conotoxin from *Conus geographus*; O, hydroxyproline.

Peptide	Sequence	pIC_{50} (95% CI)
CVID	**C**KSKGAK**C**SKLMYD**CC**TGS**C**SGTVGR**C**[b]	10.42 (±0.10)
[K10R] CVID	**C**KSKGAK**C**S**R**LMYD**CC**TGS**C**SGTVGR**C**[b]	10.81 (±0.13)
[Y13F] CVID	**C**KSKGAK**C**SKLM**F**D**CC**TGS**C**SGTVGR**C**[b]	7.79 (±0.042)
MVIIA	**C**KGKGAK**C**SRLMYD**CC**TGS**C**RS-GK**C**[b]	10.65 (±0.16)
[R10K] MVIIA	**C**KGKGAK**C**S**K**LMYD**CC**TGS**C**RS-GK**C**[b]	10.62 (±0.046)
GVIA	**C**KSOGSS**C**SOTSYNCCR-S**C**NOYTKR**C**Y[b]	10.63 (±0.17)

[a] Potency presented as the pIC_{50} ($-\log IC_{50}$) for displacement of [^{125}I]GVIA from rat brain membrane.
[b] Amidated C terminus.

TABLE II
Specificity of calcium channel antagonists to inhibit VSCC subtypes and nerve-evoked transmitter release from rat preganglionic nerve terminals
Evidence for VSCC inhibition (+), no inhibition (−), or unknown (?) are indicated. Numbers of replicate experiments (n) in the present study or reference numbers are shown.

VSCC antagonist	Transmitter release	α_{1A} (P/Q type)	α_{1B} (N-type)	α_{1C} (L-type)	α_{1E} (R-type)
ω-CVID	+ (n = 13)	− (9)	+ (n = 5) (9)	− (n = 3)	− (n = 4)
ω-MVIIA	− (n = 5)	− (9)	+ (n = 5) (9, 31)	− (n = 3)	− (n = 4)
ω-GVIA	− (n = 9)	− (29)	+ (30, 31)	− (32)	− (33)
ω-MVIIC	− (n = 5)	+ (29, 30)	+ (30)	?	− (34)
ω-agatoxin IVA	− (n = 4)	+ (29, 30)	− (30, 31)	− (32)	+ (33, 34)
ω-grammotoxin SIA	− (n = 8)	+ (30)	+ (28, 30)	− (28)	?
SNX-482	− (n = 4)	− (35)	− (28, 35)	+ (28)	+ (28, 35)
Nifedipine	− (n = 8)	− (36)	− (n = 3) (31, 36)	+ (32, 36)	− (36)

performed using acetic anhydride in *N′*,*N′*-dimethylformamide (87 μl/ml). After assembly, side chain-protecting groups were removed and the peptide was concurrently cleaved from the resin using anhydrous hydrogen fluoride/p-cresol/p-thiocresol (18:1:1). The peptides were purified and oxidized as described previously (15). Mass spectra were measured on a time-of-flight mass spectrometer (PerSeptive Biosystems) equipped with an electrospray atmospheric pressure ionization (ESI) source. Boc-L-amino acids were obtained from Auspep (Melbourne, Australia). Methylbenzhydrylamine HCl (0.79 mmol/g) was obtained from Peptide Institute (Osaka, Japan). HBTU was obtained from Richelieu Biotechnologies (Quebec, Canada). Trifluoroacetic acid, *N′*,*N′*-dimethylformamide, and *N*,*N*-diisopropylethylamine were of peptide synthesis grade and purchased from Auspep. Acetonitrile and methanol (Hypersolve Far-UV grade) were from BDH (Poole, United Kingdom). Hydrogen fluoride was supplied by Boc Gases (Brisbane, Australia). All other chemicals were of analytical grade from commercial suppliers.

^{1}H NMR Spectroscopy—All NMR spectra were recorded on a Bruker ARX 500 spectrometer equipped with a *z*-gradient unit or on a Bruker DMX 750 spectrometer equipped with a *x,y,z*-gradient unit. Peptide concentrations were ~2 mM. Hα chemical shifts for the native peptides and the two analogues were obtained from spectra recorded in 95% H_2O, 5% D_2O, pH 3.0–3.5, at 293 K. Restraints for three-dimensional structure calculations were obtained from spectra recorded at 293 K with additional experiments run at 280 K to resolve overlapping signal (15). Secondary Hα chemical shifts were analyzed compared with the random coil shift values of Wishart *et al.* (20), and structures were calculated using torsion angle dynamics/simulated annealing protocol in XPLOR version 3.8 (21–24) as previously described (14).

Drugs—Drugs were dissolved in the Krebs phosphate solution perfusing the preparation, and the effects were evaluated after they reached equilibrium (≥20 min). The dose-response relations were determined for ω-conotoxins, whereas other drugs were bath-applied at a maximally effective concentration. In addition to the synthesized ω-conotoxins, we tested ω-agatoxin IVA, ω-conotoxin GVIA, ω-conotoxin MVIIC (Alamone Laboratories, Jerusalem, Israel), SNX-482 (Peptide Institute Inc., Osaka, Japan), cadmium chloride, hexamethonium, mecamylamine, nifedipine, and tetrodotoxin (Sigma). ω-Grammotoxin SIA was a kind gift from Dr. Rick Lampe (Zeneca Pharmaceuticals, Wilmington, DE).

RESULTS

Characteristics of Excitatory Postsynaptic Potentials (EPSPs)—Stimulation of the lingual nerve with trains of stimuli (0.1–10 Hz, 4–50 V, pulse-width 0.05–0.25 ms) evoked EPSPs, which could initiate action potentials in the cell bodies of the postsynaptic neurons of the rat submandibular ganglion. The postganglionic neurons have been classified into three types by their responses to these trains of stimuli (8). In this study, neurons in which supramaximal stimulation of the preganglionic nerve fibers at 0.1 Hz either evoked a suprathreshold EPSP and action potential in response to every stimulus (strong input synapse, ≥50% of total number of neurons) (Fig. 1*A*) or where the EPSP does not usually reach threshold for the initiation of an action potential (weak input synapse, ~ 25% of neurons studied) were used. EPSPs recorded from neurons receiving either strong or weak inputs were abolished by hexamethonium (100 μM) and mecamylamine (10 μM) indicating that EPSPs were mediated by acetylcholine acting at nicotinic receptors.

Effects of Calcium Channel Inhibitors on EPSPs—ω-Conotoxin CVID produced a reversible and concentration-dependent inhibition of EPSPs (Fig. 1). Control EPSPs from both strong and weak input neurons had a mean amplitude of 26.2 ± 2.5 mV, and 20 min after bath application of CVID (100 nM), these EPSPs were reduced by 66% to a mean amplitude of 9.1 ± 1.1 mV (n = 13). The IC_{50} for inhibition of the CVID-sensitive component (79 ± 8% of peak amplitude) was 32 nM (pIC_{50} 7.5 ± 0.15). CVID had no detectable effect on the resting membrane potential of individual ganglion cells or on the amplitude and frequency of spontaneous EPSPs (n = 5) (Fig. 1, *inset*), suggesting that it acted presynaptically to inhibit neurally evoked transmitter release. To confirm that Tyr-13 in loop 2 contributes significantly to the ability of CVID to inhibit transmitter release, we assessed the potency of the phenylalanine analogue of CVID on transmitter release. [Y13F]CVID (0.1–1 μM) was without effect on the EPSPs (n = 3).

The effect of CVID contrasts with the effects of 300 nM ω-conotoxin GVIA (N-type), 100 nM ω-agatoxin IVA, 300 nM ω-conotoxin MVIIC (P/Q-type), 300 nM ω-grammotoxin SIA, 300 nM SNX-482 (R-type), and 30 μM nifedipine (L-type), which had little or no inhibitory effect on evoked and spontaneous transmitter release in rat submandibular ganglia either alone or in combination with each other (n = 3–13 per drug) (Fig. 1*D*),

confirming previous results (8). In a proportion of weak input neurons, GVIA inhibited EPSPs by up to 12% of the control amplitude (5 of 8 preparations) (Fig. 1*D*) with an IC_{50} of 60 nM, suggesting that GVIA-sensitive calcium channels play a minor role in neurotransmission in the rat submandibular ganglia. GVIA had no effect on strong input neurons ($n = 4$). EPSPs were consistently abolished by low concentrations of the non-specific calcium channel blocker Cd^{2+} (30 μM, $n = 8$), indicating that neurally evoked transmitter release from preganglionic neurons was dependent on calcium influx through VSCCs.

Of the characterized ω-conotoxins, CVID most closely resembles MVIIA in structure. Despite this structural similarity, MVIIA (10–1000 nM) failed to produce detectable inhibition of EPSPs ($n = 4$) (Fig. 2*B*). Since loop 2 contributes mostly to ω-conotoxin potency at N-type VSCCs, we investigated the influence of a Lys/Arg swap at position 10 in CVID and MVIIA on their ability to block neurotransmitter release. Bath application of a maximally effective concentration of [K10R]CVID (100 nM) produced only 19% inhibition of EPSPs (Fig. 2*A*), reducing control EPSPs of 27.6 ± 2.9 mV to 22.4 ± 2.2 mV after 20 min ($n = 8$). In contrast to the ineffective MVIIA, [R10K]MVIIA caused a 47% inhibition of EPSP amplitude (Fig. 2*C*), reducing control EPSPs from 27.0 ± 2.4 mV to 14.4 ± 2.2 mV after 20 min ($n = 6$). [R10K]MVIIA had no detectable effect on the membrane potential of individual ganglion neurons or on the amplitude and frequency of spontaneous EPSPs (data not shown), suggesting that similar to CVID, it acted presynaptically to inhibit evoked neurotransmitter release.

The effects of ω-conotoxin GVIA (100 nM), ω-agatoxin IVA (100 nM), ω-conotoxin MVIIC (100 nM), ω-grammotoxin SIA (100 nM), SNX-482 (100 nM), and nifedipine (10 μM) were also investigated on the CVID-resistant transmitter release. These toxins, applied alone or in combination with each other, had no detectable effects on the transmitter release recorded in the presence of 100 nM CVID ($n = 3$ for each toxin).

Radioligand Binding Studies—The affinity of ω-conotoxins CVID, MVIIA, and their analogues for N-type VSCCs was determined from their ability to displace [^{125}I]GVIA from rat brain membrane. The pIC_{50} values are shown in Table I. [K10R]CVID and [R10K]MVIIA had potencies that were comparable with the native peptides. However, [Y13F]CVID was significantly less potent than CVID, confirming that the hydroxyl group in Tyr-13 of CVID has a similar influence on binding to the N-type VSCC as seen previously for the Y13F analogues of GVIA and MVIIA (25).

Effect of ω-Conotoxins on Recombinant Ca^{2+} Channels Expressed in Xenopus Oocytes—The effect of ω-conotoxins CVID and MVIIA were examined on L-, N-, and R-type Ca^{2+} channels expressed in *Xenopus* oocytes. Whole cell Ca^{2+} channel currents were recorded from oocytes injected with either rat cRNA or cDNA for α_{1B}, α_{1C}, or α_{1E} in combination with $\alpha_2\delta$ and β_3 using 5 mM Ba^{2+} as the charge carrier. Bath application of either ω-conotoxins CVID or MVIIA (300 nM) inhibited the depolarization-activated inward Ba^{2+} current recorded from oocytes expressing N-type but had no effect on current through L- or R-type Ca^{2+} channels (see Table II) (29–36). The inhibition of Ba^{2+} currents through N-type Ca^{2+} channels by ω-conotoxin CVID and MVIIA was dose-dependent and slowly reversed upon washout.

Three Dimensional Structures—Hα chemical shifts relative to random coil values are a sensitive measurement of backbone conformation for disulfide-bonded isomers and can be used to locate local conformational differences across structurally related peptides (25, 26). Hα chemical shifts were similar for [K10R]CVID and [R10K]MVIIA compared with the native peptides CVID and MVIIA (Fig. 3*A*), indicating that any global

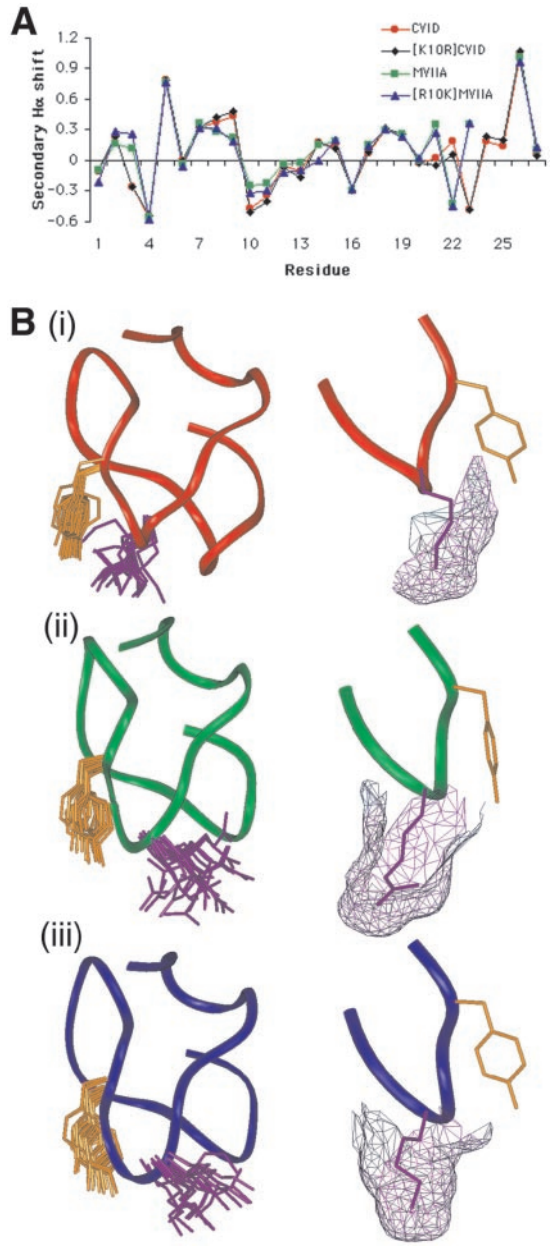

FIG. 3. **Three-dimensional structures of ω-conotoxins CVID, MVIIA, and [R10K]MVIIA.** *A*, Hα chemical shifts for ω-conotoxins CVID, [K10R]CVID, MVIIA, and [R10K]MVIIA at 293 K in 95% H_2O, 5% D_2O. Residue numbers are labeled according to the CVID sequence. *B*, ribbon diagrams of the backbones for CVID (*i*), MVIIA (*ii*), and [R10K]MVIIA (*iii*). The 17 lowest energy conformations of the side chains at positions 10 (Lys or Arg) and 13 (Tyr) are also shown on the *left side*. On the *right side* are shown the ribbon diagrams rotated 180° around the *y* axis and the calculated Connolly surface area of Lys/Arg-10 and the orientation of Tyr-13 in loop 2 (residues 8–14 are shown). Structures of the lowest energy conformation were superimposed over backbone atoms Cα, C, and N (1–27 and 1–25) for CVID, MVIIA, and [R10K]MVIIA, respectively (Insight II 2000).

structural changes on swapping residue 10 are minimal. The three-dimensional structure of [R10K]MVIIA differed from MVIIA by a root mean square deviation of 0.461 across the heavy backbone atoms, confirming the absence of any significant structural change. This is seen in the ribbon diagram showing the superimposition of the 17 lowest energy conformations and the orientation of Tyr-13 and Lys/Arg-10 for CVID, MVIIA, and [R10K]MVIIA (Fig. 3*B*). To determine whether the difference in selectivity might arise from difference surface exposure at position 10, we calculated the solvent-accessible

surface area for residue 10 over the 17–20 lowest energy conformations in Insight II. The rank order of the solvent-accessible surface area was MVIIA > [R10K]MVIIA > CVID (156 ± 8.0, 147 ± 8.1, and 92 ± 4.6 Å^2, respectively). A complete three-dimensional structure was not calculated for [K10R]CVID, because it had the same potency at the N-type VSCC and conserved Hα chemical shift differences compared with CVID especially across loop 2 (Fig. 3*A*).

DISCUSSION

Neurotransmitter release from the preganglionic cholinergic neurons innervating the rat submandibular ganglia is resistant to inhibition by commonly used selective antagonists of N-, L-, P/Q-, R-, and T-type calcium channels (8, 17). The aim of this study was to investigate the effects of the recently identified ω-conotoxin CVID, the most selective N-type *versus* P/Q-type VSCC blocker, on transmitter release from these nerve terminals. CVID (IC_{50} = 32 nM) produced up to 80% inhibition of nerve-evoked transmitter release without affecting spontaneous transmitter release, and this inhibition was reversed upon washout. In contrast, nerve-evoked transmitter release was unaffected by MVIIA (≤1 μM). Interestingly, the potency of CVID to inhibit transmitter release from preganglionic cholinergic neurons was similar to the potency of both CVID and MVIIA to inhibit N-type VSCCs in postganglionic sympathetic neurons of rat vas deferens (9).

Loop 2 of ω-conotoxins has been identified as the primary loop involved in binding to the N-type VSCC (11, 13, 25) with the hydroxyl group on Tyr-13 on both ω-conotoxin GVIA and MVIIA found to be a critical determinant of high interaction at the N-type VSCC (12, 27). The 400-fold reduction in potency of [Y13F]CVID for rat brain N-type VSCC confirmed a key role of Tyr-13 in CVID. [Y13F]CVID was also inactive on the EPSPs, indicating that N-type and CVID-sensitive VSCCs both require the hydroxyl of Tyr-13. One possible conclusion from this result is that CVID may bind to both VSCCs in a similar manner. Because loop 2 of MVIIA and CVID vary only at position 10 (Lys or Arg, respectively) (see Table. 1), we investigated the role of this position contributing to the selectivity differences observed between MVIIA and CVID by swapping these residues. [K10R]CVID (100 nM) produced significantly less (< 20%) inhibition of transmitter release than CVID, indicating that Lys-10 was the preferred residue for resistant-type VSCC inhibition by CVID. Supporting this conclusion, Lys-10 was found to markedly enhance MVIIA inhibition of resistant-type VSCCs with the [R10K]MVIIA (100 nM) causing 47% inhibition of evoked transmitter release (*i.e.* >100-fold more than MVIIA). None of the ω-conotoxins investigated affected spontaneous transmitter release or the resting membrane potential of the postsynaptic cell, indicating a selective action at presynaptic VSCCs.

The effects of the L-, N-, P/Q-, and R-type VSCC antagonists (nifedipine, ω-conotoxin GVIA, ω-conotoxin MVIIC, ω-agatoxin IVA, ω-grammotoxin SIA, and SNX-482) were investigated on the transmitter release remaining after the application of CVID. None of these VSCC inhibitors, either applied alone or in combination, had any effect on the CVID-resistant neurotransmitter release. However, the CVID-resistant release was reversibly abolished by Cd^{2+}, indicating its dependence on calcium entry into nerve terminals through VSCCs. Because the R-type VSCC inhibitors used do not inhibit all R-type VSCCs (28), we investigated the effects of ω-conotoxins CVID and MVIIA on current flow-through cloned L- or R-type calcium channels expressed in *Xenopus* oocytes. Both CVID and MVIIA had no effect on depolarization-activated Ba^{2+} currents through L- or R-type calcium channels but potently inhibited current through N-type VSCCs (see Table II) as reported previously (9).

In an attempt to understand the structural basis of the selectivity differences between ω-conotoxin MVIIA and [R10K]MVIIA at the CVID-sensitive VSCCs, we determined their secondary and tertiary structures by ^{1}H NMR. From these studies, it was evident that residue replacements at position 10 had little effect on the global fold or structure of CVID or MVIIA. However, examining the solvent-accessible surface area at position 10 revealed a trend of decreasing surface area that correlated with activity at the CVID-sensitive VSCCs in preganglionic neurons. It is possible that the degree of exposure may influence the selectivity of ω-conotoxins with the most exposed residue, Arg in MVIIA, creating a clash that precludes binding to certain VSCCs. Recently, Feng *et al.* (37) identified that a single residue change on an extracellular loop of the N-type VSCC (G1326) can influence ω-conotoxin access. Thus, relatively small differences in N-type VSCC sequence may significantly alter ω-conotoxin affinity, raising to the possibility that the VSCC targeted by CVID in preganglionic nerve terminals may be a N-type ($Ca_v2.2$) calcium channel variant that does not bind all ω-conotoxins. Two functionally distinct variants of the α_{1B} subunit, $\alpha_{1B\text{-}b}$ and $\alpha_{1B\text{-}d}$, of the N-type calcium channel that differ at two loci (four amino acids (SFMG) in IIIS3–S4 and two amino acids (Glu/Thr) in IVS3–S4) have been shown to be reciprocally expressed in rat brain and sympathetic ganglia (38). The selective expression of pharmacologically distinct VSCC splice variants of α_{1B} subunits in different regions of the nervous system is proposed to underlie the differential block of preganglionic nerve terminal VSCCs by N-type selective ω-conotoxins. Alternative splicing of the domain II–III linker region of the human N-type ($Ca_v2.2$) calcium channel α_{1B} subunit has recently been shown to differentially affect ω-conotoxin MVIIA and GVIA block of the calcium channel current (39).

In conclusion, CVID was found to be a potent inhibitor of the pharmacologically distinct VSCC controlling a major component of transmitter release in preganglionic cholinergic nerve terminals. CVID may help to define the nature and role of this VSCC. Position 10 appears to play a key role in influencing ω-conotoxin affinity for this N-type-related VSCC. Given that [^{125}I]CVID labels fewer sites in rat brain than [^{125}I]MVIIA (9), it is unlikely that these resistant-type VSCCs are among the high voltage-activated VSCCs labeled by [^{125}I]ω-Aga-IIIA in rat brain (40). Intrathecal CVID (AM336) and MVIIA (Ziconotide) are currently being evaluated clinically as treatments for severe pain (10, 41). Because parasympathetic nerves arise from spinal cord neurons, it is possible that CVID-sensitive VSCCs are also expressed and play a role in neurotransmission in the spinal cord. Given the differences in the selectivity of ω-conotoxin CVID and MVIIA for this VSCC subtype, these ω-conotoxins may have different profiles of activity in the central (for review see Refs. 10 and 42) as well as the peripheral nervous system.

REFERENCES

1. Adams, D. J., Alewood, P. F., Craik, D. J., Drinkwater, R., and Lewis, R. J. (1999) *Drug Dev. Res.* **46,** 219–234
2. Olivera, B. M., Rivier, J., Clark, C., Ramilo, C. A., Corpuz, G. P., Abogadie, F. C., Mena, E. E., Woodward, S. R., Hillyard, D. R., and Cruz, L. J. (1990) *Science* **249,** 257–263
3. Olivera, B. M., Rivier, J., Scott, J. K., Hillyard, D. R., and Cruz, L. J. (1991) *J. Biol. Chem.* **266,** 22067–22070
4. Miljanich, G. P., and Ramachandran, J. (1995) *Annu. Rev. Pharmacol. Toxicol.* **35,** 707–734
5. Gonzalez-Burgos, G. R., Biali, F. I., Cherksey, B. D., Sugimori, M., Llinás, R. R., and Uchitel, O. D. (1995) *Neuroscience* **64,** 117–123
6. Ireland, D. R., Davies, P. J., and McLachlan, E. M. (1999) *J. Physiol.* (*Lond.*) **514,** 59–69
7. Smith, A. B., and Cunnane, T. C. (1999) *Neuroscience* **94,** 891–896
8. Smith, A. B., Motin, L., Lavidis, N. A., and Adams, D. J. (2000) *Neuroscience*

95, 1121–1127
9. Lewis, R. J., Nielsen, K. J., Craik, D. J., Loughnan, M. L., Adams, D. A., Sharpe, I. A., Luchian, T., Adams, D. J., Bond, T., Thomas, L., Jones, A., Matheson, J.-L., Drinkwater, R., Andrews, P. R., and Alewood, P. F. (2000) *J. Biol. Chem.* **275,** 35335–35344
10. Smith, M. T., Cabot, P. J., Ross, F. B., Robertson, A. D., and Lewis, R. J. (2002) *Pain* **96,** 119–127
11. Kim, J. I., Takahashi, M., Ogura, A., Kohno, T., Kudo, Y., and Sato, K. (1994) *J. Biol. Chem.* **269,** 23876–23878
12. Kim, J. I., Takahashi, M., Ohtake, A., Wakamiya, A., and Sato, K. (1995) *Biochem. Biophys. Res. Commun.* **206,** 449–454
13. Lew, M. J., Flinn, J. P., Pallaghy, P. K., Murphy, R., Whorlow, S. L., Wright, C. E., Norton, R. S., and Angus, J. A. (1997) *J. Biol. Chem.* **272,** 12014–12023
14. Nielsen, K. J., Adams, D. A., Alewood, P. F., Lewis, R. J., Thomas, L., Schroeder, T., and Craik, D. J. (1999) *Biochemistry* **38,** 6741–6751
15. Nielsen, K. J., Adams, D. A., Thomas, L., Bond, T. J., Alewood, P. F., Craik, D. J., and Lewis, R. J. (1999) *J. Mol. Biol.* **289,** 1405–1421
16. Kawa, K., and Roper, S. (1984) *J. Physiol. (Lond.)* **346,** 301–320
17. Seabrook, G. R., and Adams, D. J. (1989) *Br. J. Pharmacol.* **97,** 1125–1136
18. Brock, J. A., and Cunnane, T. C. (1992) *Neuroscience* **47,** 185–196
19. Schnölzer, M., Alewood, P. F., Jones, A., Alewood, D., and Kent, S. B. H. (1992) *Int. J. Pept. Protein Res.* **40,** 180–193
20. Wishart, D. S., Bigam, C. G., Yao, J., Abildgaard, F., Dyason, H. J., Oldfield, E., Markley, J. L., and Sykes, B. D. (1995) *J. Biomol. NMR* **6,** 135–140
21. Brünger, A. T., Clore, G. M., Gronennorn, A. M., and Karplus, M. (1986) *Proc. Natl. Acad. Sci. U. S. A.* **83,** 3801–3805
22. Brünger, A. T. (1992) *A System for X-ray Crystallography and NMR. X-PLOR* version 3.1, Yale University, New Haven, CT
23. Rice, L. M., and Brünger, A. T. (1994) *Proteins Struct. Funct. Genet.* **19,** 277–290
24. Stein, E. G., Rice, L. M., and Brünger, A. T. (1997) *J. Magn. Reson.* **124,** 154–164
25. Nielsen, K. J., Schroeder, T., and Lewis, R. (2000) *J. Mol. Recognit.* **13,** 55–70
26. Gehrmann, J., Alewood, P. F., and Craik, D. J. (1998) *J. Mol. Biol.* **278,** 401–415
27. Nadasdi, L., Yamashiro, D., Chung, D., Tarczy-Hornoch, K., Adriaensesens, P., Ramachandran, J., and Nadasdi, L. (1995) *Biochemistry* **34,** 8076–8081
28. Bourinet, E., Stotz, S. C., Spaetgens, R. L., Dayanithi, G., Lemos, J., Nargeot, J., and Zamponi, G. W. (2001) *Biophys. J.* **81,** 79–88
29. Stea, A., Tomlinson, W. J., Soong, T. W., Bourinet, E., Dubel, S. J., Vincent, S. R., and Snutch, T. P. (1994) *Proc. Natl. Acad. Sci. U. S. A.* **91,** 10576–10580
30. McDonough, S. I., Boland, L. M., Mintz, I. M., and Bean, B. P. (2002) *J. Gen. Physiol.* **119,** 313–328
31. Bleakman, D., Bowman, D., Bath, C. P., Brust, P. F., Johnson, E. C., Deal, C. R., Miller, R. J., Ellis, S. B., Harpold, M. M., Han, M., and Grantham, C. J. (1995) *Neuropharmacology* **34,** 753–765
32. Tomlinson, W. J., Stea, A., Bourinet, E., Charnet, P., Nargeot, J., and Snutch, T. P. (1993) *Neuropharmacology* **32,** 1117–1126
33. Schneider T., Wei, X., Olcese, R., Costantin, J. L., Neely, A., Palade, P., Perez-Reyes, E., Qin, N., Zhou, J., Crawford, G. D., Smith, R. G., Appel, S. H., Stefani, E., and Birnbaumer, L. (1994) *Receptors Channels* **2,** 255–270
34. Stephens, G. J., Page, K. M., Burley, J. R., Berrow, N. S., and Dolphin, A. C. (1997) *Pflügers Arch. Eur. J. Physiol.* **433,** 523–532
35. Newcomb, R., Szoke, B., Palma, A., Wang, G., Chen, X., Hopkins, W., Cong, R., Miller, J., Urge, L., Tarczy-Hornoch, K., Loo, J. A., Dooley, D. J., Nadasdi, L., Tsien, R. W., Lemos, J., and Miljanich, G. (1998) *Biochemistry* **37,** 15353–15362
36. Furukawa, T., Yamakawa, T., Midera, T., Sagawa, T., Mori, Y., and Nukada, T. (1999) *J. Pharmacol. Exp. Ther.* **291,** 464–473
37. Feng, Z. P., Hamid, J., Doering, C., Bosey, G. M., Snutch, T. P., and Zamponi, G. W. (2001) *J. Biol. Chem.* **276,** 15728–15735
38. Lin, Z., Haus, S., Edgerton, J., and Lipscombe, D. (1997) *Neuron* **18,** 153–166
39. Kaneko, S., Cooper, C. B., Nishioka, N., Yamasaki, H., Suzuki, A., Jarvis, S. E., Akaike, A., Satoh, M., and Zamponi, G. W. (2002) *J. Neurosci.* **22,** 82–92
40. Yan, L., and Adams, M. E. (2000) *J. Biol. Chem.* **275,** 21309–21316
41. Brose, W. G., Gutlove, D. P., Luther, R. R., Bowersox, S. S., and McGuire, D. (1997) *Clin. J. Pain* **13,** 256–259
42. Scott, D. A., Wright, C. E., and Angus, J. A. (2002) *Eur. J. Pharmacol.* **451,** 279–286

ω-Conotoxin CVID Inhibits a Pharmacologically Distinct Voltage-sensitive Calcium Channel Associated with Transmitter Release from Preganglionic Nerve Terminals

David J. Adams, Amanda B. Smith, Christina I. Schroeder, Takahiro Yasuda and Richard J. Lewis

J. Biol. Chem. 2003, 278:4057-4062.
doi: 10.1074/jbc.M209969200 originally published online November 18, 2002
